

Classical Approximation of the Scattering Induced Wigner Correction Equation

P. Schwaha¹, O. Baumgartner¹, R. Heinzl¹, M. Nedjalkov^{1,2}, S. Selberherr¹, and I. Dimov^{2,3}

¹Institute for Microelectronics, TU Wien, Gußhausstraße 27–29, A-1040 Wien, Austria

²IPP, Bulgarian Academy of Sciences, Acad. G. Bontchev str. bl25a, 1113 Sofia, Bulgaria

³ACET Centre, University of Reading, Whiteknights P.O.Box217, Reading RG66AH, UK

E-mail: schwaha@iue.tuwien.ac.at

Abstract—Quantum simulations basically rely on two kinetic theories which account for the coherent transport at different levels of approximation. These theories have complementary properties with respect to the ability to account for de-coherence processes, and become computationally expensive in describing mixed mode transport, where both, coherent and de-coherent processes must be taken into account. We consider an approach, where the coherent information, as provided by the non-equilibrium Green's function, is used in a kind of Wigner equation for the scattering induced correction to the coherent Wigner function. Here, we address the opportunity to approximate the equation by taking the classical limit in the Wigner potential term.

I. INTRODUCTION

The nanometer and femtosecond scales of operation of modern devices give rise to a number of phenomena which are beyond purely classical description. These phenomena are classified in the International Technology Road-map for Semiconductors (ITRS, www.itrs.net) according to their importance to the performance of next generation devices. It is recognized that '... computationally efficient quantum based simulators' are of utmost interest. Quantum models capable of describing mixed mode transport, where purely coherent phenomena such as quantization and tunneling are considered along with phase breaking processes such as interactions with phonons, are especially relevant. The rising computational requirements resulting from the increasing complexity due to the mixed mode phenomena are a major concern for the development and deployment of these models. The harmony between theoretical and numerical aspects of the classical Boltzmann model is no longer among the characteristics of the quantum mechanical counterpart.

The two kinetic theories which are the foundations of quantum simulations will be sketched in the following. We first consider coherent processes. The non-equilibrium Green's function (NEGF) approach offers the most comprehensive, self-consistent way to account for correlations in space and time. However, because of numerical issues the applicability is restricted to stationary structures, basically in the ballistic limit [1]. The computational burden can be reduced by working in a mode space, obtained by separation of the problem into longitudinal and transverse directions. Furthermore, if the transverse potential profile along the transport direction remains uniform, the modes in these directions can be decoupled so that the transport becomes quasi-multidimensional.

However, this is not the case for devices with a squeezed channel or with abruptly flared out source/drain contacts which require to consider two- and three-dimensional effects [2].

One level of detail more accurate are the density matrix and the Wigner function, which are linked by the unitary Weyl-Wigner transform and which are obtained by averaging over the variable corresponding to the time correlations. The Wigner function offers many advantages due to its similarity with the classical distribution function. It has been successively applied to quasi-two-dimensional simulations [3]. An extension to a general two-dimensional transport model has already been sketched currently underway [4]. Moreover the case of transient transport is numerically admissible.

De-coherent processes destroy the correlations by breaking the spatial and temporal (related to the energy) phases [5]. In general it is a matter of particle energy which kind of correlations are more affected and thus can be neglected. For slow particles the evolution remains non-Markovian in time, while fast particles cover larger distances before feeling the de-coherent processes. If the latter are powerful enough, they destroy both types of correlations making the transport classical. As has been demonstrated [6], a gradual increase of the phonon scattering rates can almost fully destroy the coherence of the resonant-tunneling state of such a typically quantum device as a resonant tunneling diode (RTD).

Phonon interaction has been included in the NEGF formalism in a quasi-two-dimensional transport description [7]. It considerably increases the complexity of the task. Approximations are commonly needed, where the phonon self-energy terms are diagonal in the coordinate representation. This is well justified for deformation potential interaction, but must be adopted for interactions with polar phonons, surface roughness, and ionized impurities.

Phonon interaction can be easily considered by the Wigner picture due to the phase-space nature of the formalism. The Boltzmann scattering model utilized in classical simulations can be entirely applied in the quantum counterpart. Thus the Wigner equation accompanied by a Boltzmann description of the scattering processes becomes relevant with respect to the gap between purely coherent and scattering-dominated carrier transport. In the next section we consider the scattering induced Wigner correction equation (SIWCE).

II. THE SIWCE

In the case of stationary, coherent carrier transport in a one-dimensional device, the task is approached by a self-consistent Schrödinger-Poisson loop. A fully ballistic Green's function calculation yields the coherent Wigner function f_w^c [8].

$$\begin{aligned} \rho(x, x') &= -2i \int G^<(x, x', E) \frac{dE}{2\pi}; \\ f_w^c(x, k_x) &= \frac{1}{2\pi} \int ds e^{-ik_x s} \rho(x + \frac{s}{2}, x - \frac{s}{2}) \end{aligned} \quad (1)$$

The lesser Green's function $G^<$ depends on the coordinates x, x' and the energy E . The coherent Wigner function $f_w^c(x, k_x)$ is obtained from the density matrix $\rho(x_1, x_2)$ with the help of the center-of-mass transformation $x = \frac{x_1+x_2}{2}$, $s = x_1 - x_2$. Furthermore, it is assumed that under the same boundary conditions, namely the Maxwell-Boltzmann statistics, f_w^c is also a solution of the coherent Wigner equation:

$$\frac{\hbar k_x}{m} \frac{\partial}{\partial k_x} f_w^c(x, k_x) = \int dk_x' V_w(x, k_x' - k_x) f_w^c(x, k_x') \quad (2)$$

where V_w in the operator $(\mathcal{V}f_w)(x, k_x)$ on the right hand side is the Wigner potential. Scattering is accounted for by the Wigner-Boltzmann (WB) equation [9], which differs from (2) by the Boltzmann operator added to the right hand side.

$$\begin{aligned} \frac{\hbar k_x}{m} \frac{\partial}{\partial x} f_w(x, \mathbf{k}) &= \\ &\int dk_x' V_w(x, k_x' - k_x) f_w(x, k_x', \mathbf{k}_{yz}) \\ &+ \int d\mathbf{k}' f_w(x, \mathbf{k}') S(\mathbf{k}', \mathbf{k}) - f_w(x, \mathbf{k}) \lambda(\mathbf{k}) \end{aligned} \quad (3)$$

Here $S(\mathbf{k}, \mathbf{k}')$ is the scattering rate for a transition from \mathbf{k} to \mathbf{k}' and $\lambda(\mathbf{k}) = \int d\mathbf{k}' S(\mathbf{k}, \mathbf{k}')$ is the total out-scattering rate.

The coherent problem is obtained from (4) by setting the scattering rate S (and thus λ) to zero. In this case the \mathbf{k}_{yz} dependence remains arbitrary and can be specified via the boundary conditions. Formally the extrapolation must be such that $f_w^c(x, k_x')$ is recovered by the integral over \mathbf{k}_{yz} . Moreover, we want to cancel the Boltzmann scattering operator at the boundaries, where standard equilibrium conditions are assumed. Hence, a Maxwell-Boltzmann distribution $f_{MB}(k'_{yz})$ is assumed in the yz directions. This allows to uniquely augment (2) to four dimensions by introducing

$$f_w^c(x, \mathbf{k}') = f_w^c(x, k_x') \frac{\hbar^2}{2\pi m k T} e^{-\hbar^2(k_y'^2 + k_z'^2)/2mkT}$$

where the factor is the Maxwell-Boltzmann distribution $f_{MB}(k'_{yz})$ in yz directions. Finally, we introduce the correction to the homogeneous Wigner function

$$f_w^\Delta(x, k_x, \mathbf{k}_{yz}) = f_w(x, \mathbf{k}) - f_w^c(x, \mathbf{k})$$

The equation for f_w^Δ is obtained by multiplying (2) by the above factor and subtracting from the WB counterpart.

$$\begin{aligned} \frac{\hbar k_x}{m} \frac{\partial}{\partial x} f_w^\Delta(x, \mathbf{k}) &= \int dk_x' V_w(x, k_x' - k_x) f_w^\Delta(x, k_x', \mathbf{k}_{yz}) \\ &+ \int d\mathbf{k}' f_w^\Delta(x, \mathbf{k}') S(\mathbf{k}', \mathbf{k}) - f_w^\Delta(x, \mathbf{k}) \lambda(\mathbf{k}) \\ &+ \int d\mathbf{k}' f_w^c(x, \mathbf{k}') S(\mathbf{k}', \mathbf{k}) - f_w^c(x, \mathbf{k}) \lambda(\mathbf{k}) \end{aligned} \quad (4)$$

The SIWCE (4) resembles the WB equation with an additional term $f_w^{\Delta 0} = \mathcal{B}f_w^c$, which is known, as f_w^c can be obtained by Green's functions calculations. The boundary conditions cancel so that an initial condition problem is obtained with an evolution directed from in the device to the boundaries. Furthermore, by definition f_w^Δ is expected to be small, if the magnitude of the Boltzmann operator is small compared to the Wigner potential counterpart. Relevant physical conditions, where $f_w^{\Delta 0}$ is small and give rise to small scattering-induced corrections of the carrier density in RTDs, have previously been explored [8]. Here we approximate SIWCE to obtain a Boltzmann kind of equation.

III. CLASSICAL APPROXIMATION

The obtained equation is approximated by means of the classical limit.

$$\begin{aligned} \int dk_x' V_w(x, k_x' - k_x) f_w^\Delta(x, k_x', \mathbf{k}_{yz}) &= \\ - \frac{eE(x)}{\hbar} \frac{\partial f_w^\Delta(x, k_x, \mathbf{k}_{yz})}{\partial k_x} \end{aligned} \quad (5)$$

This approximation is valid for slowly varying potentials, so that the force $F(x) = eE(x)$ can only be a linear function within the spatial support of f_w^Δ . The force gives rise to Newton's trajectories

$$X(t) = x - \int_t^0 \frac{\hbar K_x(\tau)}{m} d\tau \quad (6)$$

$$K_x(t) = k_x - \int_t^0 \frac{F(X(\tau))}{\hbar} d\tau \quad (7)$$

initialized by $x, k_x, 0$. In this definition, if $t > 0$ the trajectory is called forward, otherwise it is a backward one. A backward trajectory crosses the boundary of the device at a certain time t_b , so that $f_w^\Delta(X(t_b), \mathbf{k}(t_b)) = 0$. The approximated equation can be transformed with the help of (7)

$$\begin{aligned} f_w^\Delta(x, \mathbf{k}) &= \\ \int_{t_b}^0 dt \int d\mathbf{k}' f_w^\Delta(X(t), \mathbf{k}') S(\mathbf{k}', \mathbf{k}(t)) e^{-\int_t^0 \lambda(\mathbf{k}(\tau)) d\tau} & \\ + \int_{t_b}^0 dt \left\{ \int d\mathbf{k}' f_w^c(X(t), \mathbf{k}') S(\mathbf{k}', \mathbf{k}(t)) \right. & \\ \left. - f_w^c(X(t), \mathbf{k}(t)) \lambda(\mathbf{k}(t)) \right\} e^{-\int_t^0 \lambda(\mathbf{k}(\tau)) d\tau} & \end{aligned} \quad (8)$$

into a Fredholm integral equation of the second kind with a free term given by the last two rows of (8) determined by f_w^c . The solution can be represented as a Neumann series with terms obtained by iterative application of the kernel to the free term. The series corresponds to a Boltzmann kind of evolution process, where the initial condition is given by the

free term. The genuine mixed mode problem posed by the boundary conditions is transformed into a classical evolution of the quantum-coherent solution f_w^c . The latter, however, allows negative values and thus cannot be interpreted as an initial distribution of classical electrons: rather positive and negative particles initiate the evolution process. In this way the quantum information remains in (8) by the sign of the evolving particles. The boundary is still presented by t_b , however, it has a different physical meaning: it only absorbs particles, since trajectories with evolution time $t < t_b < 0$ do not contribute to the solution. Figure 1 shows the effect of the boundaries for an equilibrium state: the histogram of the free-flight trajectories which originate at a given point and leave the simulation region increases at the boundaries indicating that fewer trajectories from these initial points contribute to the overall result. It is due to the absorbing nature of the boundaries which accordingly reduce the mean free path of the trajectories to below one half of the equilibrium value for the utilized physical model.

In very small devices the carrier dwelling time can be so small that the probability for multiple scattering events tends to zero. In such cases the initial condition f_0 itself presents the correction f_w^Δ . In all other cases the evaluation of the initial condition is a necessary step for finding the solution. The particle approach derived for this purpose is presented next.

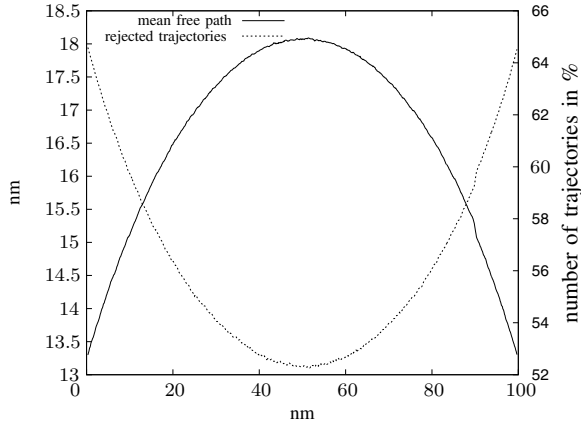


Fig. 1. Histogram of the trajectories which leave the device and mean free path for trajectories which end into the device. Equilibrium state is assumed for f_w^c , from each phase space point initiate 100 free flights.

IV. PARTICLE ALGORITHM

The computational task is specified as the calculation of the value of the two components f_{0A} and f_{0B} of the initial conditions at the given points (x^i, k_x^j) : $f_{0A}^{i,j} = f_{0A}(x^i, k_x^j)$ and the same for f_{0B} . Particle approaches are suitable for the calculation of the inner product of two functions: in our case it is the averaged value $I_{A,B}(\Omega)$ of $f_{0A,B}$ in a given domain Ω of the phase space.

$$\begin{aligned} I_{A,B} &= \int dx \int dk_x \theta_\Omega(x, k_x) f_{0A,B}(x, k_x) \\ &= \int dx \int dk_x \int dk_y \int dk_z \theta_\Omega(x, k_x) f_{0A,B}(x, \mathbf{k}) \end{aligned}$$

The domain indicator $\theta_\Omega(x, k_x)$ is 1, if its arguments belong to Ω , and 0 otherwise. Then $\Omega = \Omega^{i,j}$ can be determined by the phase space area with a small volume $\Delta = \Delta k_x \Delta x$ around (x^i, k_x^j) so that $f_{0A,B}^{i,j} = I_{A,B}(\Omega^{i,j})/\Delta$. Another peculiarity is the point wise evaluation of f_w^c giving rise to the approximation:

$$\int dx^t \int dk_x^t f_w^c(x^t, k_x^t) \simeq \sum_{i,j} f_w^c(i, j) \Delta \quad (9)$$

We focus on the contribution from the first component $f_{0A}(x, k_x)$, the second component is approached in the same fashion.

$$\begin{aligned} I_A &= \int_{-\infty}^0 dt \int dx \int dk_x \int dk_y \int dk_z \int d\mathbf{k}' \quad (10) \\ &\frac{\hbar^2}{2\pi m k T} e^{-\hbar^2(k_y'^2 + k_z'^2)/2mkT} f_w^c(X(t), k_x^t) S(\mathbf{k}', \mathbf{k}(t)) \\ &e^{-\int_t^0 \lambda(K_x(\tau), \cdot) d\tau} \theta_\Omega(x, k_x) \theta_D(X(t)) \end{aligned}$$

The lower bound of the time integral has been extended to $-\infty$, since the introduced device domain indicator θ_D takes care for its correct value at t_b . The backward parametrization of the trajectories will be changed to forward ones aiming to achieve a more heuristic picture of the evolution of the real carriers. Two important properties of the trajectories will be utilized:

- (I) Any phase space point reached by the trajectory at any given time can be used for initialization, since it obeys a system of first order differential equations. A full notation of a trajectory $X(t), K_x(t)$ contains the initialization point: $X(t) = X(t; x, k_x, 0) = x^t$, $K_x(t) = K_x(t; x, k_x, 0) = k_x^t$. Consequently, the initialization can be changed from $x, k_x, 0$ to x^t, k_x^t, t so that $x = X(0, x^t, k_x^t, t)$, $k_x = K_x(0, x^t, k_x^t, t)$.
- (II) For stationary transport the absolute clock is replaceable by a relative one: trajectories are invariant with respect to a shift of both, initialization and parametrization time.

Applying this procedure to (10), with the help of (9) results in:

$$\begin{aligned} I_A(\Omega^{n,m}) &= \sum_{i,j} \int_0^\infty dt \int dk_x^t \int dk_y \int dk_z \int d\mathbf{k}'_y z \theta_D(x_i^t) \\ &\left\{ \frac{\hbar^2}{2\pi m k T} e^{-\frac{\hbar^2(k_y'^2 + k_z'^2)}{2mkT}} \right\} f_w^c(i, j) \Delta \\ &\left\{ \frac{S(\mathbf{k}', k_x^t, k_y, k_z)}{\lambda(\mathbf{k}')} \right\} \\ &\left\{ \lambda(K_x^t(t), \cdot) e^{-\int_0^t \lambda(K_x(\tau), \cdot) d\tau} \right\} \\ &\frac{\lambda(\mathbf{k}')}{\lambda(K_x^t(t), \cdot)} \theta_{\Omega^{n,m}}(X^t(t), K_x^t(t)) \end{aligned}$$

where now \mathbf{k}' denotes $(k_{xj}, \mathbf{k}'_{yz})$. This integral has been augmented in a way that the terms in the curly brackets represent probability densities. The first bracket is the normalized Gaussian distribution, the well known probabilities for scattering and free flight can be recognized in the next two brackets. The following algorithm is obtained:

- 1) Associate to each node n, m an estimator $\xi^{n, m}$.
- 2) Loop over i, j nodes corresponding to x^t and k'_x integrals, and initiate $l = 1, 2, \dots, N$ trajectories from each node.
- 3) select the k'_{yl}, k'_{zl} values according to the term in the first curly brackets, thus accounting for the k_y, k_z integrals.
- 4) Select a wave vector according to the term in the second curly-brackets. Input parameters are $k'_{xj}, k'_{yl}, k'_{zl}$, the particular value of the after-scattering wave vector is denoted by $\mathbf{k} = k_{xl}^t, k_{yl}^t, k_{zl}^t$.
- 5) The point x_i^t, k_{xl}^t is used to initialize the trajectory $K_{xl}^t(t), X_l^t(t)$ at time $t = 0$. Then, generate a free-flight time value t_l according to the term in the last curly brackets.
- 6) Add to the estimator $\xi^{n, m}$ at the particular mesh node n, m which is nearest to the point $K_{xl}^t(t_l), X_l^t(t_l)$ the weight

$$w_l = f_w^c(i, j) \Delta \lambda(k'_{xj}, k'_{yl}, k'_{zl}) / \lambda(K_{xl}^t(t_l), k_{yl}, k_{zl})$$
- 7) At the end of the i, j loop divide $\xi^{n, m}$ by N .

V. SIMULATION EXAMPLE

The structure of the used RTD device is shown in Figure 2. The comparison of initial and corrected densities, as shown in Figure 3, shows that the scattering mechanisms increase the densities within the device compared to the purely coherent case. The present approach also revealed another peculiarity of the approach: a high sensitivity of the computations to even minor deviations from equilibrium in the contact regions. In Figure 4 only the middle part of the device is considered so that the boundary conditions correspond to the wave vector distributions at $15nm$ depth of the contacts of the genuine device. The corrected density at the left contact does not agree with the original density, which clearly violates the condition for a vanishing correction in the contacts. This effect has been observed in previous work [8], and has been associated with the lack of an accelerating field due to the applied bias in the initial condition of equation (4). This field is taken into account in the classical counterpart (8). It reveals that the effect is due to the need of a high precision – of order of 10^{-4} – for the boundary conditions. The physical effect corresponding to this effect, is that carriers in the contacts need some distance to be thermalized by the phonons.

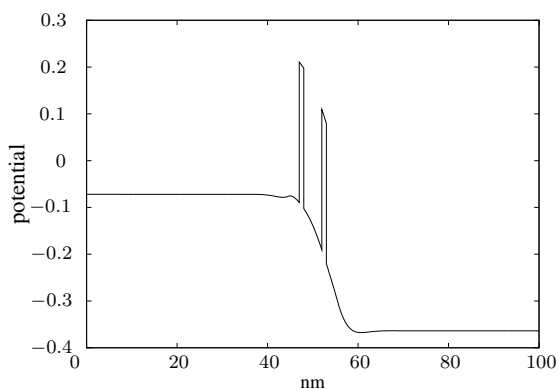


Fig. 2. Potential profile of the simulated RTD. The $4nm$ wide quantum well is surrounded by $1nm$ barriers with a height of $0.3eV$, applied is $0.3V$ bias.

ACKNOWLEDGMENT

This work has been partially supported by the Austrian Science Fund special research program IR-ON (F2509), the Austrian Science Fund project P19532-N13, and by the ÖFG, Project MOEL273.

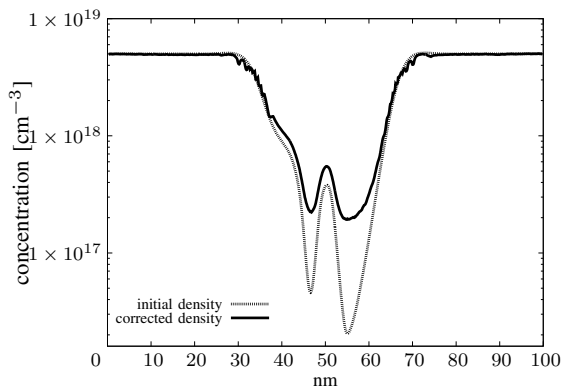


Fig. 3. Density distribution in the device under $0.3V$ bias, presented in logarithmic scale.

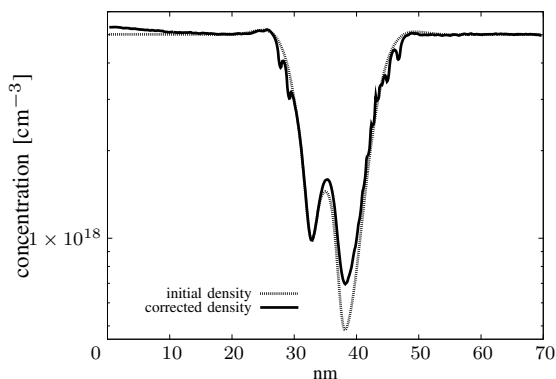


Fig. 4. An RTD with too short contact regions results in erroneous results at the contacts.

REFERENCES

- [1] R. Venugopal, *et al.*, “Simulating quantum transport in nanoscale transistors: Real versus mode space approach,” *Journal of Applied Physics*, **92**, pp. 3730–3739, 2002.
- [2] M. Luisier, *et al.* “Quantum transport in two- and three-dimensional nanoscale transistors: Coupled mode effects in the non-equilibrium Green’s function formalism”, *Journal of Applied Physics*, **100**, pp. 043713–1–043713–12, 2006.
- [3] D. Querlioz, *et al.*, “A study of quantum transport in end-of-roadmap DG-MOSFETs using a fully self-consistent Wigner Monte Carlo approach” *IEEE Trans. on Nanotechnology* **5**, p. 737-744, 2006.
- [4] M. Nedjalkov and D. Vasileska, “Semi-Discrete 2D Wigner-Particle Approach” *Journal of Computational Electronics*, **7**, p. 222-225, 2008.
- [5] M. Nedjalkov *et al.*, “Wigner Transport models of the electron-phonon kinetics in quantum wires” *Physical Review B* **74**, pp. 035311-1 – 035311-18, 2006.
- [6] D. Querlioz, *et al.*, “Wigner Monte Carlo simulation of phonon-induced electron decoherence in semiconductor nanodevices” *Physical Review B* **78**, p. 165306, 2008.
- [7] A. Svizhenko and M. P. Antram, “Role of scattering in nanotransistors,” *IEEE Trans. on Electron Devices*, **50**, pp. 1459–1466, 2003.
- [8] O. Baumgartner *et al.*, “Coupling of non-equilibrium Green’s function and Wigner function approaches”, *Proc. Simulation of Semiconductor Processes and Devices*, Hakone, Japan, pp. 931–934, 2008.
- [9] M. Nedjalkov *et al.*, “Unified Particle Approach to Wigner-Boltzmann Transport in Small Semiconductor Devices” *Physical Review B* **70**, p. 115319, 2004.